INTERNATIONAL JOURNAL FOR NUMERICAL AND ANALYTICAL METHODS IN GEOMECHANICS, VOL. 20, 231–252 (1996)

AN INTERFACE MODEL TO DESCRIBE VISCOPLASTIC BEHAVIOR

NARESH C. SAMTANI

Senior Geotechnical Engineer, Parsons Brinckerhoff Quade & Douglas, Inc. One Penn Plaza, New York, NY 10119, U.S.A.

CHANDRA S. DESAI

Regents' Professor, Department of Civil Engineering and Engineering Mechanics, University of Arizona, Tucson, AZ 85721, U.S.A.

AND

LAURENT VULLIET

Professor, Department of Civil Engineering, École Polytechnique Fédérale De Lausanne, CH-1015 Lausanne, Switzerland

SUMMARY

A constitutive model to describe viscoplastic or time-dependent behaviour of interface materials is presented. Viscoplastic characteristics of the interface material are modeled based on Perzyna's theory of viscoplasticity and the Hierarchical Single Surface (HiSS) series of constitutive models. Experiments performed using a new interface test device to characterize the behaviour of cohesive soil–rock interfaces are described. Procedures to derive model parameters are presented together with validation of the model. Finite element implementation of the interface element is described along with verification of the model with respect to field behaviour of a creeping natural slope.

KEY WORDS: interfaces and joints; landslides; viscoplastic behavior; hierarchical single surface models; laboratory testing; calibration; finite element method; validations

INTRODUCTION

An interface is the plane of contact that exists between two neighbouring bodies which can be treated as a thin smeared zone. In context of civil engineering, interfaces can occur at junctions or contact between structures and various geologic media, between various structural elements or between various geologic formations. Figure 1 shows several examples where behaviour of interfaces can significantly affect the overall system response.

Appropriate modeling of the behaviour of interface materials is a subject of considerable importance in engineering because of relative movements at interfaces. One of the major considerations in engineering analysis and design is the variation of the states of stresses and strians with time. Proper representation of stress–strain time behaviour of materials, particularly interfaces, can be crucial in defining the long-term behaviour of many systems, such as those shown in Figure 1.

Although a number of investigators have proposed mechanistic idealizations and constitutive models for interfaces (see review below), none appear to allow consideration of factors such as

CCC 0363–9061/96/040231–22

Received 13 March 1995
Revised 22 August 1995

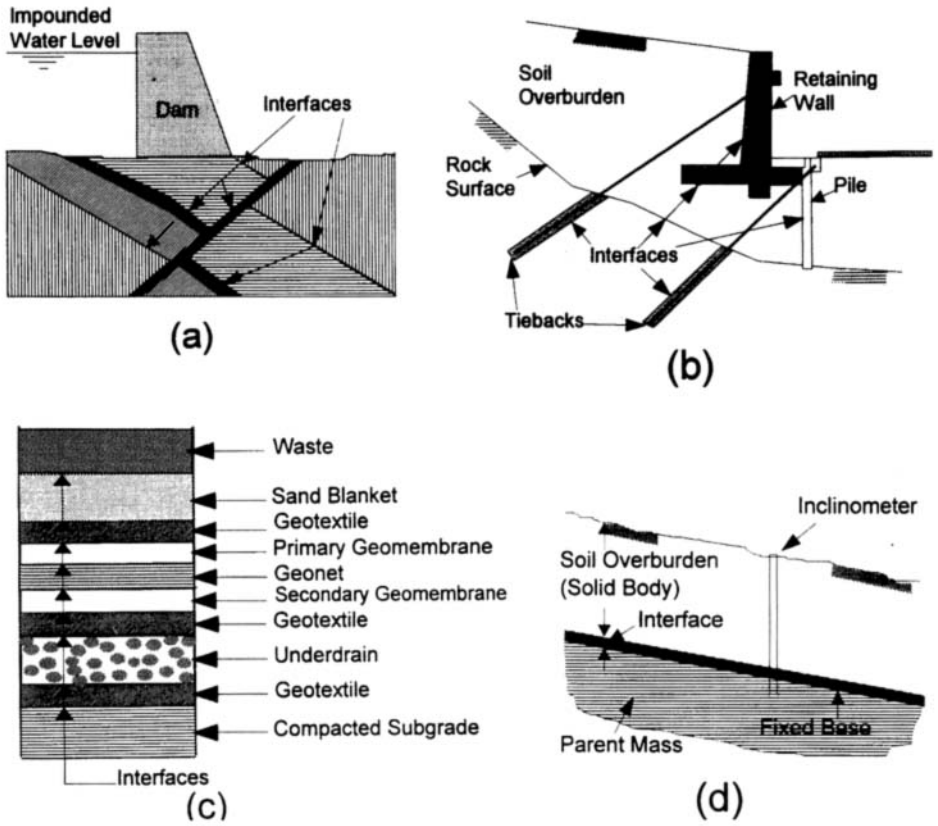

Figure 1. Examples of interfaces: (a) gravity dam on an inclined and stratified rock formation; (b) an underpinned and tied-back retaining wall; (c) cross-section of a typical landfill liner system; (d) a creeping natural slope

elastic, plastic and viscous (time-dependent) deformations, volume changes and stress paths in the constitutive models, in a unified manner. The objectives of this paper are: (1) to present such a unified constitutive model for interfaces, (2) to calibrate the model and determine its parameters from a set of laboratory tests, (3) to validate the model with respect to viscoplastic behaviour observed in laboratory tests and (4) to illustrate the capability of the model by introducing it in a non-linear finite element procedure and verifying the model with respect to field and experimental data.

REVIEW OF LITERATURE

Both analytical and experimental studies have been undertaken in recent yers to understand and describe the influence of interface behaviour. Earlier interface formulations ranged from considering interfaces in the form of pin connections between two bodies to a complex assembly of springs and dashpots to simulate translational and rotational motions in soil–structure interaction problems.[1,2] With the advancement of numerical procedures such as the finite element method, interfaces have been represented by various types of one-, two- and three-dimensional elements. A comprehensive review of interface models has been presented by Desai.[3] In the following, a few relevant studies in which finite elements were used to model interfaces are reviewed.

The most commonly used elements in the interaction problem are based on the joint element concept proposed by Goodman *et al.*[4] This is essentially a one-dimensional (1-D) line element with finite length and zero thickness. Later on, this element was extended to have a (small) finite thickness. For example, Zienkiewicz *et al.*[5] developed a two-dimensional (2-D) element based on the isoparametric concept while Ghaboussi *et al.*[6] presented a 2-D element model which used relative displacements as independent degrees of freedom. These 1-D and 2-D elements were further researched and used in linear and non-linear interaction analysis by various workers.[7-12] The 2-D element was extended to a three-dimensional (3-D) element for 3-D linear and non-linear analysis of the soil–structure problems.[13,14] In these formulations, the interface behaviour was represented by uncoupled normal and shear responses. The shear behaviour was simulated as non-linear elastic or plastic and the shear stiffness was evaluated as a tangent modulus from laboratory stress–strain behaviour in direct shear tests. The normal stiffness, on the other hand, was arbitrarily assigned a high value to prevent overlap of neighboring bodies.

In order to realistically define the interface normal and shear responses including the coupling thereof, Desai *et al.*[3,15] proposed the concept of the thin element (2-D or 3-D) in which the interface behaviour was considered as a problem in constitutive modelling. In this concept, an appropriate constitutive model was used to realistically describe the behaviour of interface materials and develop the stiffness matrix for finite element implementation. Such constitutive modelling of the interface materials allows appropriate stress distribution between the interface zones and the surrounding media. As a result, phenomena such as remolding and degradation in the interface zones can be readily incorporated. This element, also known as the *thin layer interface element*, has been shown to be versatile and its two-dimensional version has been intensively researched to describe the elastic and elastoplastic behaviour of interface materials.[3,15-18] Since the formulation of this element is essentially the same as solid elements, it is easier to program and implement in numerical procedures.

None of the above models allow for time-dependent behaviour of interfaces. Basd on the concept of the thin layer interface element, this paper presents an interface model in which the elastic, plastic and viscous behaviour of interface materials are considered in a unified manner.

INTERFACE MODEL FRAMEWORK

Formulation

The interface behaviour involves primarily shear deformation under normal stress, σ_n, and shear stress, τ as shown in Figure 2(a). The dominant deformation pattern observed in many interfaces involves a simple shear strain condition as shown in Figure 2(b), wher u and v are deformations in the local x and y co-ordinate directions, while u_r and v_r are relative shear and normal displacements, respectively.

For use in numerical procedures such as the finite element and finite difference procedures, the interface can be represented by a 6-noded rectangular element with a width, B, and thickness, t as shown in Figure 2(c). A simple shear condition is represented for the case of equal displacements of the top nodes and equal displacements of the bottom nodes. This can be written as

$$\begin{aligned} u_3 = u_4 = u_6 = u_t, \qquad & u_1 = u_2 = u_5 = u_b \\ v_3 = v_4 = v_6 = v_t, \qquad & v_1 = v_2 = v_5 = v_b \end{aligned} \tag{1}$$

where the subscripts 1 to 6 represent the six nodes while subscripts t and b represent the top and bottom nodes of the interface. In such a case only normal and shear strains occur, as the in-plane

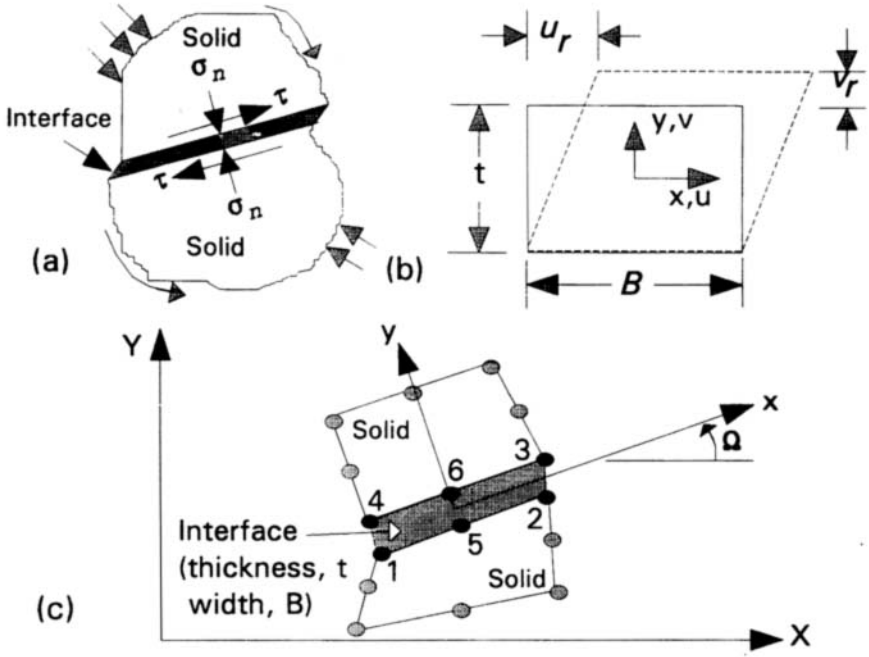

Figure 2. Formulation of interface model: (a) schematic of an interface; (b) idealized simple shear strain deformation mode for interfaces; and (c) six-node interface element

deformation (i.e., along the direction of B) is zero. Thus, we can write,

$$\varepsilon_{xx} \simeq 0, \qquad \varepsilon_{yy} = v_r/t, \qquad \gamma_{xy} = u_r/t \tag{2}$$

where $u_r = u_t - u_b$ and $v_r = v_t - v_b$ are the relative displacements in the x and y directions, respectively. In equation (2), ε_{yy} represents the normal strain ε_n, and γ_{xy} represents the shear strain ε_s of the interface. Thus, if the in-plane strain ε_{xx} is assumed to be zero or negligible,[19] i.e., when simple shear conditions are approximately satisfied, the local strain vector $\{\varepsilon'\}$ can be written as

$$\{\varepsilon'\} = \begin{Bmatrix} \varepsilon_n \\ \varepsilon_s \end{Bmatrix} = \begin{Bmatrix} v_r/t \\ u_r/t \end{Bmatrix} \tag{3}$$

where the superscript ℓ denotes local system. In incremental form, the relative displacements can be represented in terms of strain components as

$$\begin{Bmatrix} dv_r \\ du_r \end{Bmatrix} = \begin{bmatrix} t & 0 \\ 0 & t \end{bmatrix} \begin{Bmatrix} d\varepsilon_n \\ d\varepsilon_s \end{Bmatrix} \tag{4}$$

Since $\varepsilon_{xx} \simeq 0$, we have $\sigma_{xx} \simeq 0$; hence, the local stress vector $\{\sigma'\}$ can be written as

$$\{\sigma'\} = \begin{Bmatrix} \sigma_{yy} \\ \sigma_{xy} \end{Bmatrix} = \begin{Bmatrix} \sigma_n \\ \tau \end{Bmatrix} \tag{5}$$

where the components are effective stresses. These effective stresses $\{\sigma'\}$ are related to the relative displacements, V_r and u_r in incremental form as

$$\begin{Bmatrix} d\sigma_n \\ d\tau \end{Bmatrix} = \begin{bmatrix} C_{11} & C_{12} \\ C_{21} & C_{22} \end{bmatrix} \begin{Bmatrix} dv_r \\ du_r \end{Bmatrix} \tag{6}$$

where C_{11} and C_{22} are related to normal and shear stiffnesses while C_{12} and C_{21} represent coupling effects between the normal and shear behaviour.

Substitution of equation (4) into equation (6) gives

$$\begin{Bmatrix} d\sigma_n \\ d\tau \end{Bmatrix} = t \begin{bmatrix} C_{11} & C_{12} \\ C_{12} & C_{22} \end{bmatrix} \begin{Bmatrix} d\varepsilon_n \\ d\varepsilon_s \end{Bmatrix} \tag{7a}$$

or

$$\{d\sigma'\} = [\bar{C}']\{d\varepsilon'\} \tag{7b}$$

where $[\bar{C}']$ is the interface constitutive matrix at the local level. Transformation of the above relations to a general global frame-invariant form is presented later. One of the contributions of this paper is to define $[\bar{C}']$ which describes the elastic, plastic and viscous response of interface materials in a unified manner. The elasto-viscoplastic model used to define $[\bar{C}']$ is described next.

Elasto-viscoplastic model

The proposed elasto-viscoplastic model is based on the assumption of small strains wherein the total strain vector, $\{\dot{\varepsilon}'\}$, is decomposed into elastic, $\{\dot{\varepsilon}'_e\}$, and viscoplastic, $\{\dot{\varepsilon}'_{vp}\}$, parts as follows:

$$\{\dot{\varepsilon}'\} = \{\dot{\varepsilon}'_e\} + \{\dot{\varepsilon}'_{vp}\} \tag{8}$$

where the overdot denotes time rate. The elastic behaviour is assumed independent of time; therefore, $\{\dot{\varepsilon}'_e\} = \{\varepsilon'_e\}$. Furthermore, if the shear and normal responses are assumed to be decoupled, then the elastic behaviour of the interface can be expressed as follows:

$$\{\varepsilon'_e\} = \begin{Bmatrix} \varepsilon_{en} \\ \varepsilon_{es} \end{Bmatrix} = \begin{bmatrix} tk_n & 0 \\ 0 & tk_s \end{bmatrix} \begin{Bmatrix} \sigma_n \\ \tau \end{Bmatrix} \tag{9a}$$

where subscripts n and s denote normal and shear components, and k_n and k_s are the elastic normal and shear stiffness of the elastic interface materials which are expressed as follows:

$$k_n = \frac{d\sigma_n}{dv_r}, \qquad k_s = \frac{d\tau}{du_r} \tag{9b}$$

The viscoplastic strain rate vector, $\{\dot{\varepsilon}'_{vp}\}$, is based on Perzyna's theory of viscoplasticity[20] and is expressed as follows:

$$\{\dot{\varepsilon}'_{vp}\} = \Gamma \left\langle \Phi\left(\frac{F}{F_0}\right) \right\rangle \left\{ \frac{\partial Q}{\partial \sigma'} \right\} \tag{10a}$$

or

$$\begin{Bmatrix} \dot{\varepsilon}_{vpn} \\ \dot{\varepsilon}_{vps} \end{Bmatrix} = \Gamma \left\langle \phi\left(\frac{F}{F_0}\right) \right\rangle \begin{Bmatrix} \dfrac{\partial Q}{\partial \sigma_n} \\ \dfrac{\partial Q}{\partial \tau} \end{Bmatrix} \tag{10b}$$

where ϕ a scalar flow function of the yield function F, F_0 is a normalizing constant having the same units as F, Q is a viscoplastic potential and Γ is a material parameter which is also known as the fluidity parameter. Time dependency is introduced through Γ which has the units of inverse time. By analogy with plasticity, associative viscoplasticity is defined by $Q \equiv F$. The angle bracket $\langle\ \rangle$ has the meaning of a switch-on–switch-off operator; when $F/F_0 > 0$, $\langle\phi(F/F_0)\rangle = \phi(F/F_0)$, and when $F/F_0 < 0$, $\langle\phi(F/F_0)\rangle = 0$.

In Eqs. (10a) and (10b), any plasticity based constitutive model can be adopted. Herein, the constitutive model derived from the generalized Hierarchical Single Surface (HiSS) series of models is used.[18] For this model, the F and Q functions are as follows:

$$F = \tau^2 + \alpha\sigma_n^{\bar{n}} - \gamma\sigma_n^2 = 0 \tag{11a}$$

$$Q = \tau^2 + \alpha_Q\sigma_n^{\bar{n}} - \gamma\sigma_n^2 \tag{11b}$$

where τ and σ_n are nondimensionalized with respect to atmospheric pressure, p_a. The parameter $\bar{n}$ is related to the transition point at which the normal displacement transits from compression to dilation, α is the hardening function expressed in terms of plastic strain trajectories, α_Q is a function to control dilative behavior of materials and is expressed in terms of α, and the parameter γ is related to the slope of the ultimate envelope for F when $\alpha = 0$. A continuous surface is given by F (Figure 3).

Model features

The proposed elasto-viscoplastic material model can be characterized by the following:

(i) There are only elastic deformations and no time-dependent (viscoplastic) deformations if the stress state is inside the yield surface.
(ii) A state outside the yield surface will generate viscoplastic strains. This increases the amount of accumulated viscoplastic strains, modifies the value of the hardening function,

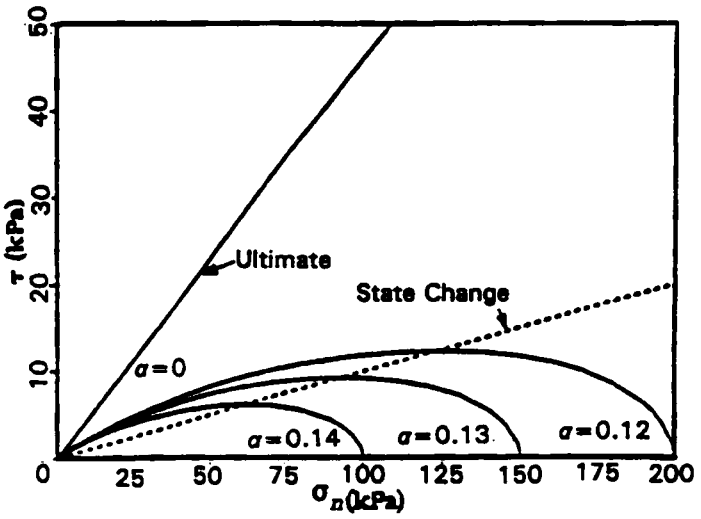

Figure 3. Plot of yield function F

and as a result changes the position of the yield surface F. When F passes through the stress point, then deformations cease.

(iii) Any stress point lying between the current yield surface F and the ultimate surface (given by $\alpha = 0$ in the above constitutive model) will provoke a transient creep phenomenon. When the steady-state condition is reached, the solution obtained from the inviscid plasticity model is obtained.

(iv) A stress point outside of the ultimate surface will provoke a secondary creep response (constant strain rate). Zienkiewicz and Cormeau[21] have pointed out that in the context of limit analysis, the solution obtained when the movements stop is a lower bound while the solution obtained when the movements continue at a constant rate is an upper bound.

These characteristics are valid for any hardening based plasticity model. Herein, as mentioned before, the constitutive model based on the HiSS approach is used.

MODEL FOR NORMALLY CONSOLIDATED CLAYS

The proposed elasto-viscoplastic model was applied for understanding the phenomenon of creeping natural slopes in normally consolidated cohesive soils.[22] A creeping natural slope generally involves the slow movement of a large soil mass over a relatively stationary parent material. An interface zone of finite thickness occurs near the junction of the moving soil mass and the underlying stationary or parent mass, Figure 1(d). Figure 4 shows a schematic of a typical displacement profile recorded by inclinometers in creeping natural slopes. It is observed that in the interface zone the variation of translational displacement is much more severe than that in the mass above the interface zone.[22,23] The pattern of these movements is similar to a simple shear strain deformation mode. The rate of movement is largely controlled by the viscous characteristics of the interface material. This section briefly describes an experimental study to simulate the deformation behaviour in such slopes and calibration of the proposed viscoplastic model.

Two sets of tests were performed, namely static interface tests and undrained creep tests. The purpose of the static interface tests was to derive the model parameters and hardening functions for the plasticity based portion of the proposed model [equations (11a) and 11(b)] while the undrained creep tests permitted determination of appropriate flow functions and creep parameters [equations 10(a) and 10(b)].

Testing was performed on soil obtained from a creeping natural slope at Villarbeney, Switzerland.[22–24] The soils at this site are normally consolidated with average water content of 20 per cent, plastic limit of 20 per cent, liquid limit of 40 per cent, dry unit weight of 18.5 kN/m^3, clay fraction of 35 per cent, specific gravity of solids of 2·66; it is classified as CL.

Static interface tests

The interface tests were conducted in the new version of the Cyclic Multi Degree Of Freedom (CYMDOF) device for interfaces and joints which was originally conceived and designed by Desai over the last decade or so. The early version involved testing under dry conditions.[3,16–18] The recent version involves cylindrical interfaces and allows for fluid pressures and introduces a number of improvements.

The cross-section of the shear test specimen is shown in Figure 5.[22,25,26] The parent mass on which the slide is occurring was represented by a rigid soft rock specimen while the soil representing the sliding mass was contained in a stack of circular teflon coated aluminum rings which offer lateral confinement and allow simple shear deformations. The internal diameter of the

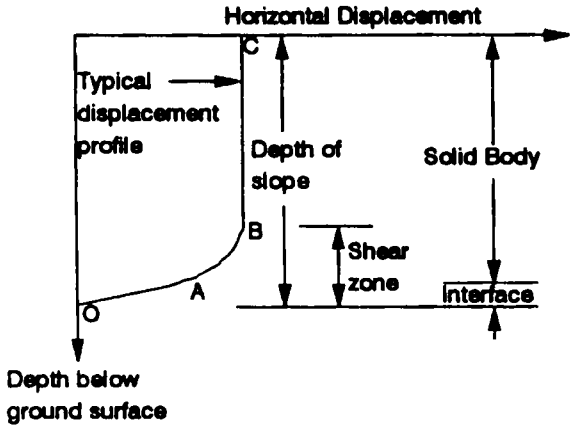

Figure 4. Typical displacement profiles observed from inclinometric measurements in creeping natural slopes

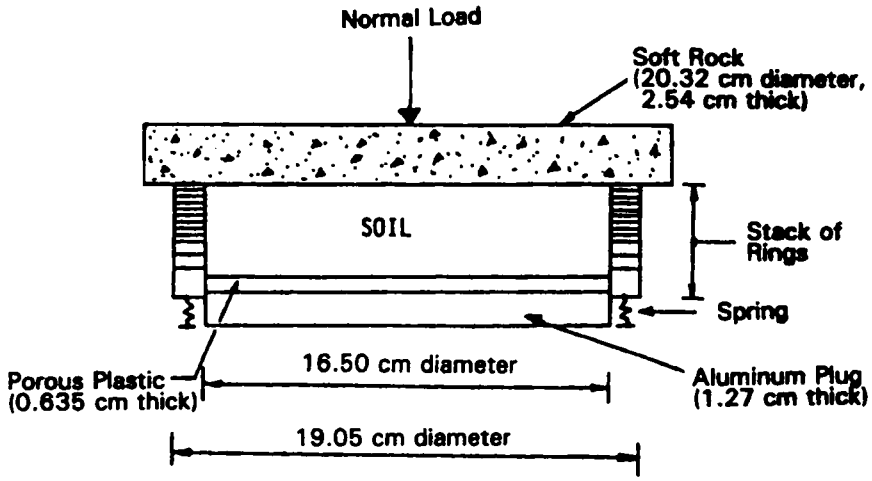

Figure 5. Cross-section of interface test set-up

rings was 16·5 cm while the total thickness of the soil specimen in the rings was 3·6 cm. The effect of overburden was simulated by applying normal loads. Shear was imposed by subjecting the soft rock specimen to prescribed displacements. Loads and displacements were applied using a hydraulic system and were monitored by load cells and Linear Variable Differential Transformers (LVDT). An electronic data collection/control system was used to collect data. Details about the testing apparatus and its calibration are presented elsewhere.[22, 25, 26]

Drained interface tests at various normal stresses and shear amplitudes were conducted. Normal stresses, σ_n, of 103, 207 and 345 kPa were used to simulate a range of overburden stresses in the creeping natural slope at Villarbeney. After the samples were consolidated under the normal stresses, they were sheared under drained conditions with different amplitudes of shear displacements, $u_r^a = 0{\cdot}19, 0{\cdot}64$ and $1{\cdot}27$ cm. Thus, large shear strains up to about 35 per cent were allowed.

To avoid build-up of excess pore pressures and to simulate drained conditions typically found in creeping natural slopes, a slow rate of shear displacement of 0·0127 mm/min was adoped for all the tests based on guidelines developed by Gibson and Henkel.[27] Dissipation of excess pore pressures took place by radial drainage provided by the rings and axial drainage provided by the porous plastic at the base of the soil sample and to some extent by the soft rock specimen. The assembly of the solid plug beneath the porous plastic and the spring elements ensured a constant normal stress at all times during shear by allowing the entire system to adjust for the vertical deformation of the soil due to drainage during shear.

Figure 6 shows results for an interface test conducted at a normal stress of 207 kPa at an amplitude of 0·64 cm. Similar behaviour is observed for tests conducted at other normal stresses. The test results were corrected for the friction between various components of the device and their stiffness such as the friction between the shear rings and the stiffness of the spring elements. Details of these corrections are given by Samtani and Desai.[22]

All tests showed a monotonic increase in shear strength and a monotonic decrease in the volume (vertical displacement). Both the shear strength and the vertical displacement approach a finite ultimate state. This hardening or yielding behaviour can be described by the following hardening function, α:

$$\alpha = \frac{\gamma \exp(-a\xi_{vpv})}{(1 + \xi_{vpd})^b} \tag{12}$$

where ξ_{vpv} and ξ_{vpd} are lengths of the volumetric and deviatoric plastic strain trajectories, respectively, and a and b are (positive) material parameters. In addition, to properly represent the volume reduction during shear, the following function for α_Q is proposed to allow for possible non-associative response:

$$\alpha_Q = \alpha + \alpha_{ph}\left[1 - \frac{\alpha}{\alpha_i}\right]^{\kappa} \tag{13}$$

where $\alpha_{ph} = (2/\bar{n})\gamma\sigma_n^{2-\bar{n}}$ and $\alpha_i = \gamma\sigma_n^{2-\bar{n}}$ are values of α at the transition or state change point and at the beginning of shear loading, respectively, and κ is a non-associative parameter.

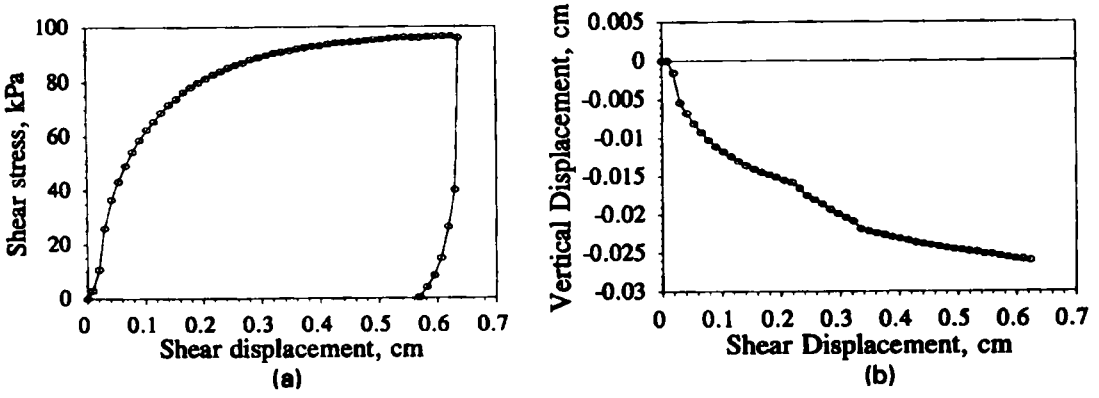

Figure 6. Results of interface test at σ_n = 207 kPa, u_r^a = 0·64 cm

Creep tests

To define the viscous behaviour, a series of undrained shear strain creep tests with pore water pressure measurements performed by Vulliet[23] on the same clay were used. To simulate the conditions within the interface in the creeping natural slope at Villarbeney, the tests were conducted with normal stress, σ_n, of 200 and 400 kPa, and constant shear stress, τ, such that the stress ratio τ/σ_n was 0·6 and 0·8, respectively. A subsequent figure (Figure 12) shows typical test results in terms of shear strain vs. time for $\tau/\sigma_n = 0{\cdot}6$. Based on experimental data, the following commonly used flow function[21,22,28,29] was found to be appropriate for the Villarbeney clay

$$\left\langle \phi\left(\frac{F}{F_0}\right)\right\rangle = \left(\frac{F}{F_0}\right)^N \tag{14}$$

where N is a material parameter which together with Γ defines the viscous behaviour.

PROCEDURE FOR DETERMINATION OF MODEL PARAMETERS

Three sets of parameters are required to define the elasto-viscoplastic interface behavior. These are elastic, plastic and viscous parameters. The elastic behaviour of interface requires the elastic normal stiffness, k_n, and elastic shear stiffness, k_s [equation (9b)]. The plastic part of interface behaviour can be categorized into associative and non-associative. Description of the associative model requires the definition of the yield function F [equation (11a)], and the evolution or hardening function α [equation (12)]. Thus, the required parameters are γ, $\bar{n}$ and the hardening function parameters a and b. The non-associative model requires, in addition to the definition of the associative model, the plastic potential function Q [equation (11b)], and its evolution rule defined by α_Q [equation (13)], therefore, in this case, the non-associative parameter κ is required. To define the viscous behaviour the viscous parameter Γ [equation (10b)] and N [equation (14)] are needed. Thus, altogether nine parameters are required to present the elasto-viscoplastic interface behaviour with the non-associative flow rule. The procedure for the determination of these parameters is presented below.

(1) Elastic parameters, k_n, k_s

The normal stiffness of an interface can be determined from tests in which the normal displacements of the interface under normal stress are measured. The shear stiffness is determined from the interface simple shear tests. The slopes of the unloading curves obtained from these tests give values of k_n and k_s, respectively, Figure 7.

(2) Plastic paraemters, γ, $\bar{n}$, a, b, and κ

Ultimate (or failure) parameter γ: The ultimate shear stress condition of the interface is given by $\alpha = 0$ in the yield function F [equation (11a)]; hence,

$$\frac{\tau_p}{\sigma_n} = \sqrt{\gamma} \tag{15}$$

where τ_p is the peak shear stress for a given normal stress σ_n. The square of the slope of the τ_p vs. σ_n curve will give γ, Figure 8. The plot shown in Figure 8 is similar to that used for determination of the internal friction angle from the conventional Mohr–Coulomb criterion.

Transition parameter $\bar{n}$: The interface tests conducted here showed a monotonic decrease in volume. In this model, when the volume respnse is completely contractive, a value of $\bar{n} > 2$ can be assumed; here, a value of $\bar{n} = 2{\cdot}04$ is assumed.

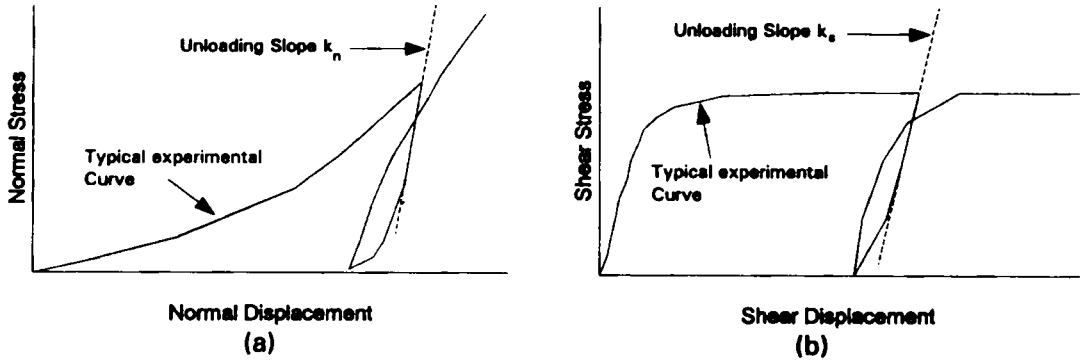

Figure 7. Elastic parameters: (a) determination of k_n; (b) determination of k_s

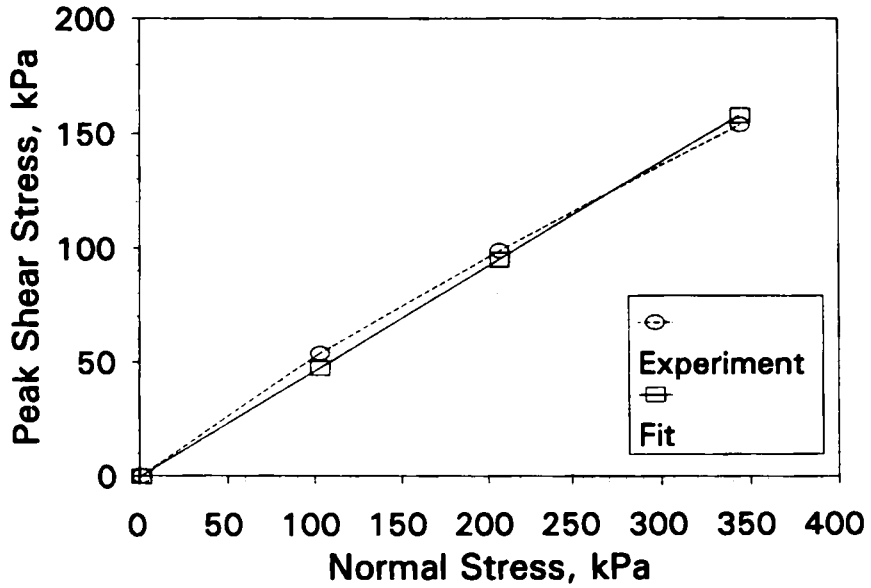

Figure 8. Determination of ultimater parameter γ

Hardening parameters a, b: Equation (12) can be rewritten as follows:

$$a\xi_{vpv} + b \ln \xi_{vpd} = \ln \gamma - \ln \alpha \tag{16}$$

The values of α in equation (16) for various stress states (σ_n, τ) are compured from $F = 0$ [equation (11a)]. Thus, i number of data points will give i number of linear simultaneous equations to be solved for two unknowns a and b. A least-squares method is used to calculate a and b.

Non-associative parameter κ: Equation (13) can be rewritten as follows:

$$\ln\left(\frac{\alpha_Q - \alpha}{\alpha_{ph}}\right) = \kappa \ln\left(1 - \frac{\alpha}{\alpha_i}\right) \tag{17}$$

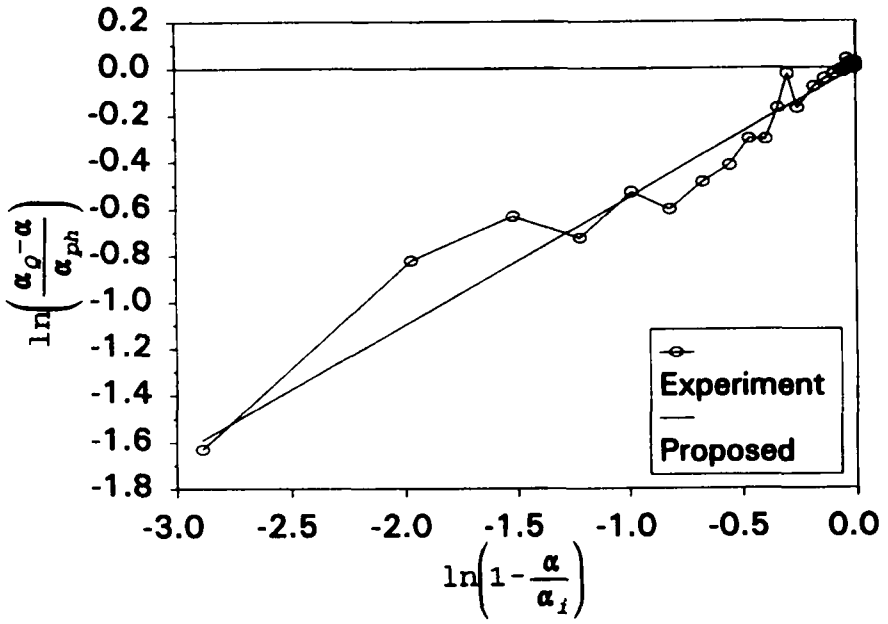

Figure 9. Determination of non-associative parameter κ from interface test conducted at $\sigma_n = 207$ kPa

The values of α_Q at various data points are computed using equation (11b) and substituted in equation (17). A graph $\ln[(\alpha_Q - \alpha)/\alpha_{ph}]$ vs. $\ln(1 - \alpha/\alpha_i)$ is then plotted. Figure 9 shows a typical plot corresponding to the interface test conducted at $\sigma_n = 207$ kPa. The slope of the average straight line on this plot gives the value of κ.

(3) Viscous parameters, Γ and N:

Equation (10a) can be rewritten as follows:

$$\Gamma\left\langle \phi\left(\frac{F}{F_0}\right)\right\rangle = \chi, \quad \text{where } \chi = \sqrt{\left(\frac{\{\dot{\varepsilon}'_{vp}\}^T\{\dot{\varepsilon}'_{vp}\}}{\{\partial Q/\partial\sigma'\}^T\{\partial Q/\partial\sigma'\}}\right)} \tag{18}$$

where superscript T denotes a transposed vector. Substitution of equation (14) in to equation (18) leads to

$$\Gamma\left(\frac{F}{F_0}\right)^N = \chi \tag{19}$$

which on taking the logarithm gives

$$\ln\Gamma + N\ln(F/F_0) = \ln(\chi) \tag{20}$$

The values of χ and (F/F_0) are computed from laboratory creep tests at all data points, and a plot of $\ln(F/F_0)$ vs. $\ln(\chi)$ is obtained; a schematic is shown in Figure 10(a). The intercept along $\ln(\chi)$, say c, gives the value of Γ ($= \exp C$) and the slope of the average straight line gives the value of N. Figure 10(b) shows determination of creep parameters from a simple shear creep test for a sample preconsolidated at 200 kPa and tested under a stress ratio of 0·6.

Based on the above procedures, the parameters were determined from all interface and creep tests. An average set of parameters was then determined and is summarized in Table I.

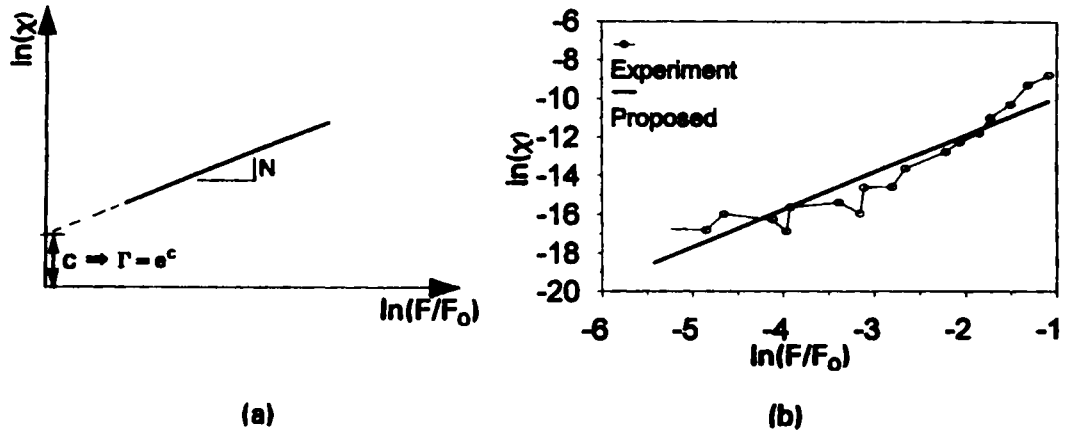

Figure 10. Viscous parameters: (a) schematic plot of $\ln(F/F_0)$ vs. $\ln(\chi)$; (b) determination of viscous parameters from a simple shear creep test conducted under a stress ratio of 0·6 for a sample preconsolidated to 200 kPa

Table I. Parameters for interface model

Parameters	Symbol	Value
Elastic		
Normal stiffness	k_n	8×10^6 kPa/cm
Shear stiffness	k_s	2800 kPa/cm
Plastic		
Ultimate	γ	0·24
Transition	$\bar{n}$	2·04
Hardening	a	143·0
Hardening	b	10·0
Nonassociative	κ	0·57
Viscous		
Fluidity	Γ	0·057/min
Exponent	N	3·15

VALIDATION OF CONSTITUTIVE MODELS

The constitutive models were validated by backpredicting laboratory tests used to find the constants and independent tests not used for finding the constants. The validation was based on numerical integration of the stress–relative displacement relationship and viscoplastic law presented earlier; details are given by Samtani and Desai.[22] Typical results are presented here. These results were obtained by using the average parameters presented in the Table I. Additional verifications of the interface model in boundary value problems are presented later.

Figure 11 shows comparisons between backpredictions and test data for the interface test conducted at $\sigma_n = 103$ kPa. Figure 12 shows comparisons for the simple shear creep test for two samples preconsolidated at 200 and 400 kPa, and tested under the same stress ratio of 0·6. These results show that the proposed constitutive model provides satisfactory characterization of the elastoplastic and elastoviscoplastic behaviour of interfaces.

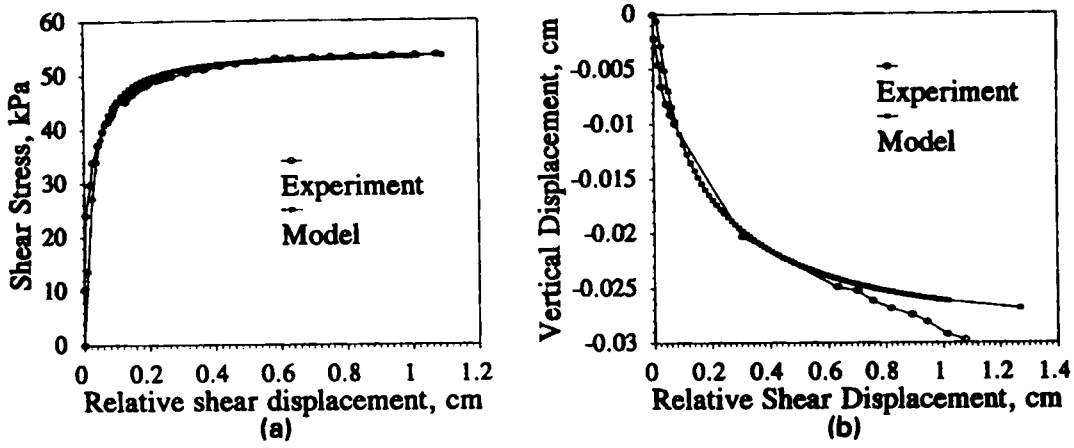

Figure 11. Comparisons between predictions and observations for interface test at $\sigma_n = 103$ kPa

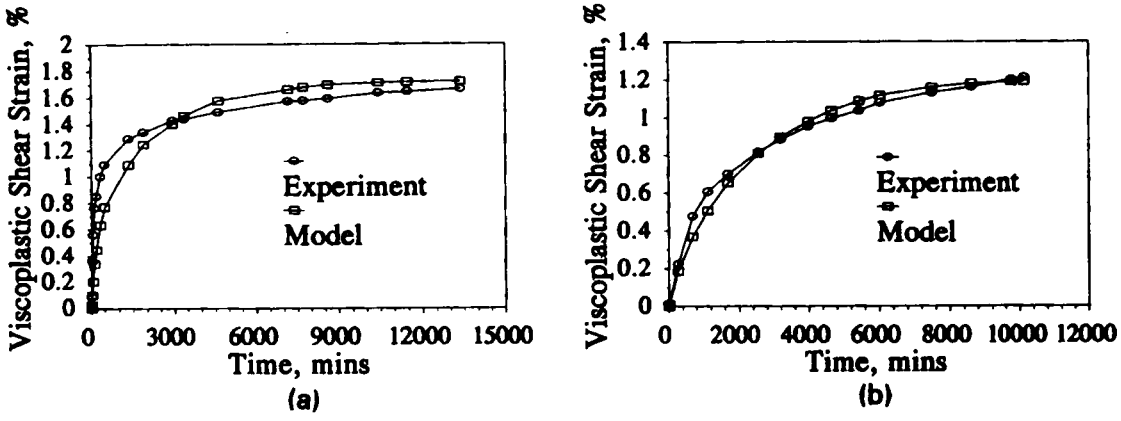

Figure 12. Comparisons between prediction and observation for creep tests, stress ratio = 0·6: (a) preconsolidation stress = 200 kPa; (b) preconsolidation stress = 400 kPa

IMPLEMENTATION IN FINITE ELEMENT ANALYSIS

Finite element formulation of a boundary value problem is performed in a global co-ordinate system (X, Y). Very often in such problems, the local co-ordinate system (x, y) of the interface element is inclined at an angle, say Ω, with respect to the horizontal in the global system, Figure 2(c). Furthermore, in the global formulation the stress–strain and stiffness matrices are expressed in general 3-D terms. Thus, in order to implement the interface model in a finite element code, it is necessary to account for the arbitrary inclination and also to transform the stress–strain relation [equation (7)] for interfaces from the local (x, y) co-ordinate system to a generalized frame-invariant relation in the global co-ordinate system (X, Y).[19] The global representation is presented next followed by a brief description of the finite element viscoplastic algorithm.

Global representation of interface formulation

Plane strain conditions are used to illustrate the transformation of the interface model from the local system to a global system. Let $\{dS\}$ and $\{dE\}$ represent the incremental stress and strain vectors in the global (X, Y) system and $\{d\sigma\}$ and $\{d\varepsilon\}$ represent the incremental stress and strain vectors in the local (x, y) co-ordinate system. The various components of these vectors are expressed as follows:

Global:

$$\{dS\}^T = [dS_{XX}, dS_{YY}, dS_{XY}] \tag{21a}$$

$$\{dE\}^T = [dE_{XX}, dE_{YY}, dE_{XY}] \tag{21b}$$

Local:

$$\{d\sigma\}^T = [d\sigma_{xx}, d\sigma_{yy}, d\sigma_{xy}] \tag{22a}$$

$$\{d\varepsilon\}^T = [d\varepsilon_{xx}, d\varepsilon_{yy}, d\varepsilon_{xy}] \tag{22b}$$

The transformation of these vectors from local to global description and *vice versa* is given by,

Local to global:

$$\{dS\} = \{\varpi'\}\{d\sigma\} \tag{23a}$$

$$\{dE\} = \{\varpi\}\{d\varepsilon\} \tag{23b}$$

Global to local:

$$\{d\sigma\} = \{\Theta'\}\{dS\} \tag{24a}$$

$$\{d\varepsilon\} = \{\Theta\}\{dE\} \tag{24b}$$

where

$$[\varpi'] = \begin{bmatrix} 0 & CS & -2CS \\ 0 & C^2 & 2CS \\ 0 & -CS & C^2 - S^2 \end{bmatrix}, \quad [\varpi] = \begin{bmatrix} 0 & CS & -CS \\ 0 & C^2 & CS \\ 0 & -2CS & C^2 - S^2 \end{bmatrix}$$

$$[\Theta'] = \begin{bmatrix} 0 & 0 & 0 \\ S^2 & C^2 & -2CS \\ -CS & CS & C^2 - S^2 \end{bmatrix}, \quad [\Theta] = \begin{bmatrix} 0 & 0 & 0 \\ S^2 & C^2 & -CS \\ -2CS & 2CS & C^2 - S^2 \end{bmatrix}$$

In the above matrices, $C = \cos\Omega$ and $S = \sin\Omega$. In addition to accounting for the arbitrary inclination of the interface element, these transformation matrices also express the local stress–strain relation in the general 3-D configuration. The latter is done by using zeros in the first column of $[\varpi]$ and $[\varpi']$ and in the first row of $[\Theta]$ and $[\Theta']$ which yield $d\varepsilon_{xx} \simeq 0$ and $d\sigma_{xx} \simeq 0$, respectively, to represent simple shear strain conditions. Using the above transformation matrices, the global constitutive matrix, $[\bar{C}]$, can be written as follows:

$$[\bar{C}] = [\varpi][\bar{C}'][\varpi']^T \tag{25}$$

The above global constitutive matrix, $[\bar{C}]$, can now be conveniently used to find the global stiffness matrix of the whole system. Thus, it can be seen that only the transformation of the local constitutive matrix is required to obtain the global stiffness matrix, whereas in other formulations[4] transformation of the local (interface) stiffness matrix is required to obtain the global stiffness matrix.

Finite element viscoplastic algorithm

A brief description of the finite element viscoplastic algorithm is presented here.[28,30] The viscoplastic strain at a given time step n is evaluated from equation (10a). The viscoplastic strain rate at step $n+1$ can be obtained by using Taylor's series, ignoring the higher-order terms in Δt^n as

$$\{\dot{\varepsilon}_{vp}^{n+1}\} = \{\dot{\varepsilon}_{vp}^{n}\} + \left[\frac{\partial \dot{\varepsilon}_{vp}}{\partial \sigma}\right]^n \{\Delta\sigma^n\} = \{\dot{\varepsilon}_{vp}^{n}\} + [G^n]\{\Delta\sigma^n\} \tag{26}$$

where $\{\Delta\sigma^n\}$ is the vector of stress increment, and $[G^n]$ denotes the gradient at n. The viscoplastic strain increment, $\{\Delta\varepsilon_{vp}^n\}$, during a time interval $\Delta t^n = t^{n+1} - t^n$ can be written as

$$\{\Delta\varepsilon_{vp}^n\} = \Delta t^n[(1-\theta)\{\dot{\varepsilon}_{vp}^n\} + \theta\{\dot{\varepsilon}_{vp}^{n+1}\}] \tag{27}$$

where θ can assume different values, e.g., $\theta = 0$ gives the explicit (Euler) time-integration scheme.

The incremental stress vector $\{\Delta\sigma^n\}$ can be written as

$$\{\Delta\sigma^n\} = [\bar{C}^n]\langle[B]\{\Delta q^n\} - \{\dot{\varepsilon}_{vp}^n\}\Delta t^n\rangle \tag{28}$$

where $[B]$ is the strain–displacement transformation matrix, $\{\Delta q\}$ is the vector of incremental nodal displacement and

$$[\bar{C}^n] = [[I] + [C^e]\langle\theta\Delta t^n[G^n]\rangle]^{-1}[C^e] \tag{29}$$

is referred to as the elasto-viscoplastic constitutive matrix. In equation 29, $[C^e]$ is the elastic matrix while $[I]$ is the unit matrix. The expressions for the various components of the elasto-viscoplastic matrix at the local level are presented in Appendix I.

The equations of equilibrium to be satisfied at any instant of time t^n, can be written in incremental form as follows:

$$\int_V [B]^T\{\Delta\sigma^n\}\,dV = \{\Delta Q^n\} \tag{30}$$

where $\{\Delta Q^n\}$ is the incremental vector of applied nodal loads. Use of equation (28) leads to

$$[k_t^n]\{\Delta q^n\} = \{\Delta\bar{Q}^n\} \tag{31}$$

where

$$[k_t^n] = \int_V [B]^T[\bar{C}^n][B]\,dV \tag{32}$$

is the tangential stiffness matrix,

$$\{\Delta\bar{Q}^n\} = \int_V [B]^T([\bar{C}^n]\{\dot{\varepsilon}^n_{vp}\}\Delta t^n)\,dV + \{\Delta Q^n\} \tag{33}$$

is the modified nodal loads vector, and

$$\int_V [B]^T([\bar{C}^n]\{\dot{\varepsilon}^n_{vp}\}\Delta t^n)\,dV = \int_V [B]^T(\Delta\sigma)\,dV \tag{34}$$

represents the current body load which includes body load contributed from each time step. Once the increments of stresses and strains are computed, the total quantities at time t^{n+1} can be found as

$$\{\sigma^{n+1}\} = \{\sigma^n\} + \{\Delta\sigma^n\} \tag{35a}$$

$$\{q^{n+1}\} = \{q^n\} + \{\Delta q^n\} \tag{35b}$$

$$\{\varepsilon^{n+1}\} = \{\varepsilon^n\} + \{\Delta\varepsilon^n\}. \tag{35c}$$

This process is repeated at each time step until the stresses at all Gauss points satisfy $F \simeq 0$. Since the process is incremental, residual out-of-balance forces are obtained from each time step which are then added to the applied load increment at the next time step.

The time step was selected subject to following empirial criteria:[21]

$$\Delta t^n \leqslant \rho\sqrt{\frac{I_2}{\dot{I}_2^{vp}}}; \quad \Delta t^{n+1} \leqslant \Psi\Delta t^n \tag{36}$$

where I_2 and $\dot{I}_2^{vp}$ are the second invariants of the strain and inelastic strain-rate tensors, respectively, and ρ and ψ are specified time-step control constants. The first criterion selects a variable time-step size such that the change of strain occurring during the next time interval is a fraction of the total strain accumulated before. The second criterion imposes a restriction on the variable step size between successive intervals calculated by the first criterion to prevent oscillations in solutions as steady-state conditions are approached.

VERIFICATION OF PROPOSED INTERFACE MODEL

The verification of the proposed model with respect to field observations for interfaces in creeping natural slopes is presented here. For verification, an existing two-dimensional finite element program, SSTIN (an acronym for Soil–Structure Interaction), prepared by Desai and co-workers for elasto-plastic analysis was modified for elasto-viscoplastic analysis using the algorithm presented earlier. The procedure was based on the small-strain theory which was used as an approximation for the problem of creeping natural slopes; however, it may be noted that large strains and displacements can potentially occur in such slopes. Six-noded isoparametric elements were used to represent interfaces. In addition, to represent the continuum or bodies surrounding the interface elements, 8-node isoparametric elements were implemented in this program using a similar viscoplastic algorithm. A 2×2 numerical integration scheme was utilized for both the 8-node and 6-node elements.

Field observations in the form of inclinometer data were available at three locations on the creeping natural slope at Villarbeney, Switzerland.[23,24] Figure 13 shows recorded measurements

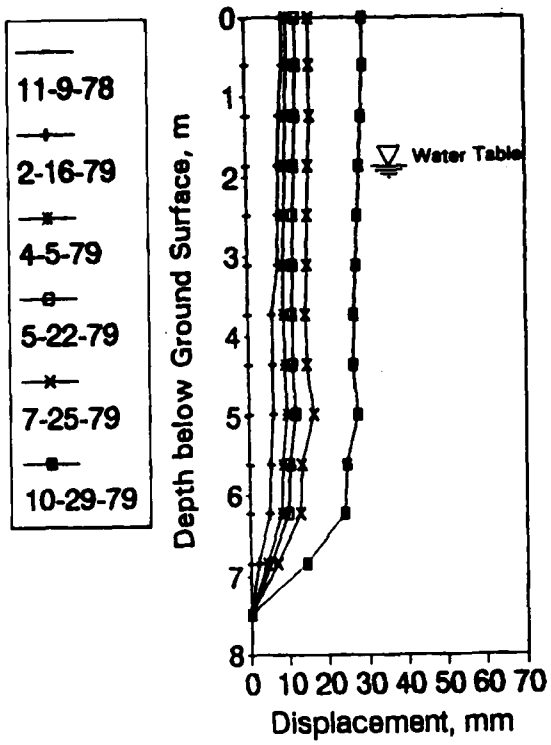

Figure 13. Observed inclinometric profiles at borehole E_2

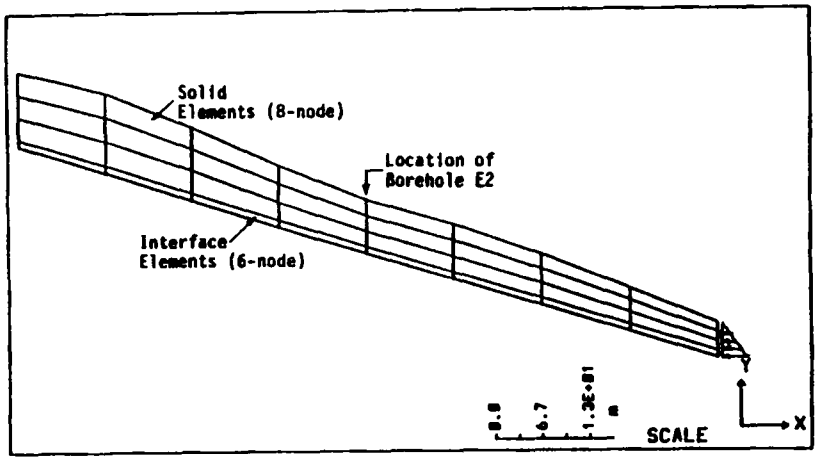

Figure 14. Finite element mesh for borehole E_2

from one of the inclinometers, labeled E_2, which was located in the central region of the slope and sufficiently far away from the edges. The base inclination of the sliding mass at this location was found to be 17°. Based on piezometric measurements in boreholes it was found that the ground-water level was about 2 m below the ground surface and did not vary significantly during

the time period of approximately one year considered herein; these observations indicate steady-state seepage conditions which are typical for such creeping slopes.

Plane strain conditions were assumed as a reasonable approximation since the location E_2 is far away from the edges of sliding mass. Figure 14 shows a finite element discretization for a length of 50 m on either side of location E_2; thus, a total of 100 m length was considered for analysis. This mesh contains 132 nodes with 8 six-noded interface elements and 24 eight-noded elements to represent the sliding soil mass. Based on field data (Figure 13) the thickness of the interface element was adopted to be 1·0 m. Since higher-order isoparametric elements were used for the soil and interface elements, it was possible to adopt a relatively coarse mesh. It was found that further refinement of the mesh did not yield significant improvements in computed results.[24]

Both vertical and horizontal displacements were restrained at the base. The left-hand bondary was free to move, while end tractions corresponding to 75 per cent of the limiting Coulomb passive earth pressure were applied at the right-hand boundary to simulate the natural earth pressur within the creeping slope.[31] Based on a sensitivity study, it was found that variation of these tractions within a range of 50–100 per cent of the passive pressure results in minor variations in the predictions presented herein.

The seepage forces corresponding to steady-state conditions were found from a flow net analysis and were superimposed on those due to the weight of the soil. The initial conditions involved introduction of the *in situ* state of stress assuming normal consolidation including the effects of hydrostatic pressure, zero strains, and zero strain rates.

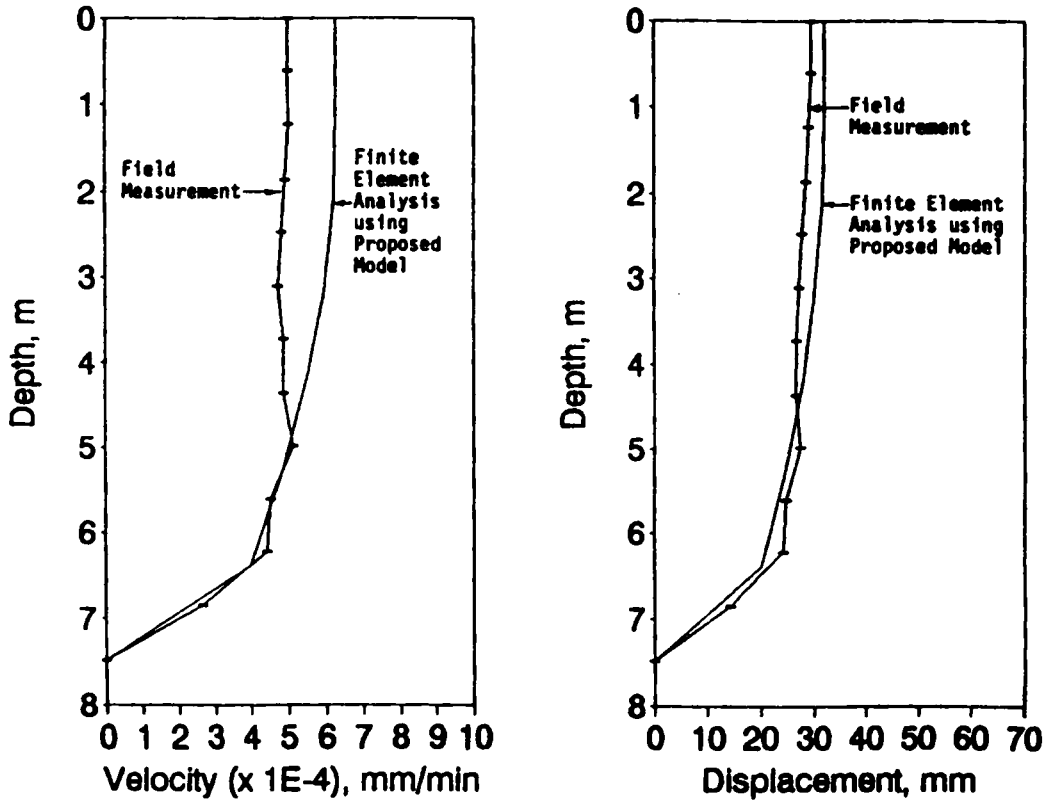

Figure 15. Comparisons of predictions and observations at borehole E_2: (a) velocity; (b) displacement

The interface model proposed herein with parameters listed in Table I was used to simulate the response of interface materials. The behaviour of soil mass overlying the interface was characterized by an elasto-viscoplastic model based on the generalized HiSS model; details of this model are presented elsewhere.[22,24]

An arbitrary smal time step of 10 min was used to initiate time-stepping. Subsequent time steps were selected based on the variable time-stepping scheme given by equation (36) with values of $\rho = 0.02$ and $\psi = 1.2$. The solution was continued until the viscoplastic strain rate reached a steady condition at the integration points in the elements; this was identified when the viscoplastic strain rate was small ($< 10^{-9}$ /min). To achieve this strain rate, approximately 9200 progressively larger time steps were required. On a 486–33 Mhz computer, the solution was achieved in approximately 35 min.

Figure 15 shows typical finite element results after a period of 354 days in comparison with the field observations for inclinometer E_2. Here the velocity was obtained by dividing the difference in displacements by the corresponding time increment when the steady viscoplastic strain rate was reached. The predictions based on the proposed interface model compare very well with the observed velocity and displacement profiles.

CONCLUSIONS

The proposed interface model permits simultaneous description of elastic, plastic, and viscous responses of interface materials. It is conceptually simple and involves a minimal number of parameters to describe each response. The model is constructed in a modular fashion in the sense that it can be easily used to describe purely elastic or purely elastic responses of interfaces as special cases.

A series of experiments conducted in a new interface device have been described. Procedures for determination of model parameters have been presented. Finite element implementation of the model is presented. Since the formulation of the interface element is similar to other solid finite elements, it is easier to program and implement.

It has been shown by verifications with respect to experimental data and boundary value problems that the model is versatile and can satisfactorily characterize interface materials. Based on this study, it is believed that the proposed model can provide a satisfactory and consistent formulation of interface behaviour under long-term conditions. Furthermore, the proposed formulation can allow for such factors as remolding or degradation of interface materials as it considers stress redistribution effects and permits consideration of time-dependent responses of neighbouring bodies as well.

Although the small-strain theory presented in this paper can be used as a reasonable approximation, for a general formulation it would be appropriate and desirable to include large strains and displacements.

ACKNOWLEDGEMENT

Part of the research herein was supported by grant No. MSM 8618901/14 from the National Science Foundation, Washington D. C. The provision of clay from Villarbeney by Dr. E. Recordon, Soil Mechanics Laboratory, Swiss Federal Institute of Technology, Lausanne, Switzerland is appreciated. Useful discussions with Prof. K.G. Sharma of Indian Institute of Technology, New Delhi, India, are gratefully acknowledged. The authors wish to acknowledge considerable assistance from Dr. D. Rigby towards the use of CYMDOF device.

APPENDIX I

The general elasto-viscoplastic matrix, $[\bar{C}^{ep}]$, for an interface element at time step n, at the local level for any constitutive model can be explicitly written as follows.[22]

$$[\bar{C}^{ep}] = \begin{bmatrix} k_n \dfrac{1 + \theta \Delta t^n k_s G^n_{22}}{|C^n_{eg}|} & k_s \dfrac{-\theta \Delta t^n k_n G^n_{12}}{|C^n_{eg}|} \\ k_n \dfrac{-\theta \Delta t^n k_s G^n_{22}}{|C^n_{eg}|} & k_s \dfrac{1 + \theta \Delta t^n k_n G_{11}}{|C^n_{eg}|} \end{bmatrix} \tag{37}$$

where G^n_{11}, G^{nm}_{12}, G^n_{21} and G^n_{22} are the elements of the matrix $[G^n]$, k_n and k_s are the normal and shear stiffnesses, respectively, and

$$|C^n_{eg}| = [1 + \theta \Delta t^n k_n G^n_{11}][1 + \theta \Delta t^n k_s G^n_{22}] - (\theta \Delta t^n) k_n G^n_{12} k_s G^n_{21} \tag{38}$$

Equation (37) is transformed to global level using equation (25) which is then used in equation (28). Specific equations for the HiSS model [equation (11a) and (11b)] are presented by Samtani and Desai.[22] For the explicit time-integration scheme $\theta = 0$, the above relations give the elastic behaviour.

REFERENCES

1. H. W. Anderson and J. S. Dodd, 'Finite element method applied to rock mechanics', *Proc. 1st Cong. Int. Soc. for Rock Mech.*, Lisbon, Portugal, 1966.
2. D. Ngo and A. C. Scordelis, 'Finite element analysis of reinforced concrete beams', *ACI J.*, **64**, 3 (1967).
3. C. S. Desai, 'Behavior of interfaces between structural and geologic media', a state-of-the-art paper, *Int. Conf. Recent Advances in Geotech. Earthquake Eng. and Soil Dyn.*, St. Louis, Missouri, 1981.
4. R. E. Goodman, R. L. Taylor and T. L. Brekke, 'A model for the mechanics of jointed rock', *J. Soil Mech. Found. Div.* ASCE, **98**, 399–422 (1968).
5. O. C. Zienkiewicz, B. Best, C. Dullage and K. G. Stagg, 'Analysis of nonlinear problems in rock mechanics with particular reference to jointed rock systems', *Proc. 2nd Congr. on the Int. Soc. for Rock Mech.*, Belgrade, Vol. 3, 1970, pp. 501–509.
6. J. Ghaboussi, E. L. Wilson and J. Isenberg, 'Finite element for rock joint and interfaces', *J. Soil Mech. Found. Div. ASCE*, **99**, 833–848 (1973).
7. G. W. Clough and J. M. Duncan, 'Finite element analyses of retaining wall behavior', *J. Soil Mech. Found. Div. ASCE*, **97**, (1971).
8. M. G. Katona *et al.* 'CANDE — a modern approach for the structural design and analysis of buried culverts', *Report No. FHWA-RD-77-J*, Federal Highway Administration, Washington D.C., 1976.
9. L. R. Herrmann, 'Finite element analysis of contact problems', *J. Eng. Mech. Div. ASCE*, **104**, 1043–1057 (1978).
10. G. N. Pande and K. G. Sharma, 'On joint/interface elements and associated problems on numerical illconditioning', Short Communications, *Int. J. Numer. Analyt. Methods Geomech.*, **3**, (1979).
11. J. Isenberg and D. K. Vaughan, 'Nonlinear effects in soil–structure interaction', *Proc. Symp. on Implementation of Comp. Procedures and Stress–Strain Laws in Geotech. Eng.*, Chicago, 1981, 29–44.
12. N. C. Samtani, J.-N. Wang, F. Pepe and M. J. Abrahams, 'Horizontal and vertical movements of bridge piers subjected to ship impact', *Proc. SETTLEMENT '94 Conf. on Vertical and Horizontal Deformations of Foundations and Embankments — ASCE Geotechnical Special Publication No. 40*, College Station, Texas, Vol. 1, 1994, 245–256.
13. C. S. Desai and G. C. Appel, 'Three-dimensional analysis of laterally loaded structures', *Proc. Second Int. Conf. Num. Methods in Geomech. ASCE*, Virginia Tech., Blacksburg, Virginia, 1976, pp. 405–418.
14. C. S. Desai, H. V. Phan and J. V. Perumpral, 'Mechanics of three-dimensional soil–structure interaction', *J. Eng. Mech. Div. ASCE*, **100**, 731–747 (1982).
15. C. S. Desai, M. M. Zaman, J. G. Lightner and H. J. Siriwardane, 'Thin-layer element for interfaces and joints', *Int. J. Numer Analyt. Methods Geomech.*, **8**, 19–43 (1984).
16. M. M. Zaman, C. S. Desai and E. C. Drumm, 'An interface model for dynamic soil–structure interaction', *J. Geotech. Eng. Div. ASCE*, **110**, 1257–1273 (1984).
17. C. S. Desai and B. K. Nagaraj, 'Modeling for cyclic normal and shear behavior of interfaces', *J. Eng. Mech. ASCE*, **114**, 1198–1217 (1988).
18. C. S. Desai and K. L. Fishman, 'Plasticity based constitutive model with associated testing for joints', *Int. J. Rock Mech. Monthly Sci.*, **28**, 15–26 (1991).

19. K. G. Sharma and C. S. Desai, 'Analysis and implementation of thin-layer element for interfaces and joints', *J. Eng. Mech. ASCE*, **118**, 2442–2462 (1992).
20. P. Perzyna, 'Fundamental problems in viscoplasticity', *Adv. Appl. Mech.*, **9**, 243–377 (1966).
21. O. C. Zienkiewicz and I. C. Cormeau, 'Visco-plasticity–plasticity and creep in elastic soids — a unified numerical solution approach', *Int. J. Numer Methods Engrg.*, **8**, 821–845 (1974).
22. N. C. Samtani and C. S. Desai, 'Constitutive modeling and finite element analysis of slowly moving landslides using the hierarchical viscoplastic material model', *Report to National Science Foundation*, Department of Civil Engrg. and Engrg. Mech., University of Arizona, Tucson, Arizona, 1991.
23. L. Vulliet, 'Modèlisation des pentes naturelles en mouvement', *Thèse No. 635*, Ecole Polytechnique Fèdèrale de Lausanne, Lausanne, Switzerland, 1986.
24. C. S. Desai, N. C. Samtani and L. Vulliet, 'Constitutive modeling and analysis of creeping slopes', *J. Geotech. Engrg. ASCE*, **121**, 43–56 (1995).
25. C. S. Desai and D. B. Rigby, 'Cyclic interface shear test device with pore pressure measurement', *J. Geotech. Eng., ASCE*, (1995) submitted.
26. D. B. Rigby and C. S. Desai, 'Cyclic shear device for interfaces and joints with pore water pressure', *Report to National Science Foundation*, Department of Civil Engrg. and Engrg. Mech., University of Arizona, Tucson, Arizona, 1988.
27. R. E. Gibson and D. J. Henkel, 'The influence of duration of tests at constant rate of strain on measured 'drained' strength', *Geotechnique*, **4**, 6–15 (1954).
28. C. S. Desai and D. Zhang, 'Viscoplastic model for geologic materials with generalized flow rule', *Int. J. Numer. Analyt. Meth. Geomech.*, **11**, 603–620 (1987).
29. M. G. Katona and M. A. Mulert, 'A viscoplastic cap model for soils and rocks', in C. S. Desai and R. H. Gallagher, *Mechanics of Engineering Materials*, Chapter 17, Wiley, New York, 1984, pp. 335–349.
30. D. R. Owen and E. Hinton, *Finite Elements in Plasticity: Theory and Practice*, Pineridge Press Ltd., Swansea, U.K. 1980.
31. G. Ter-Stepanian and H. Ter-Stepanian, 'Back analyses for determining the Landslide pressure on a bridge abutment', *Proc. Fifth Int. Symp. on Landslides*, Lausanne, Switzerland, 1988, pp. 331–336.